ISSN: 2538-2152; ECOPERSIA 2027;15(1):37-54.

# Combining Bivariate Statistical and Expert-Based Approaches for Landslide Susceptibility Assessment

**ARTICLEINFO**

***Article Type***
**Original Research**

***Authors***
Majid Mohammady, *Ph.D.*[*]

**How to cite this article**
Mohammady M. Combining Bivariate Statistical and Expert-Based Approaches for Landslide Susceptibility Assessment. ECOPERSIA 2027;15(1): 37-54.

**DOI:**
10.48311/ecopersia.2026.121731.82927

[1] Associate Professor, College of Natural Resources, Semnan University, Semnan, Iran.

**ABSTRACT**

**Aims:** Landslides are natural hazards that are increasingly influenced by human activities. These events increase sediment input into river systems, changing sediment transport. This study's main methodological contribution is integrating a bivariate model (Information Value) with an expert-based approach (AHP) to account for the relative importance of conditioning factors in landslide susceptibility mapping.

**Material & Methods:** First, a landslide distribution map was prepared. Eleven factors, including lithology, slope angle, elevation, aspect, clay content, soil pH, distance to roads, faults, rivers, land-use, and rainfall, were incorporated into the model. The relative importance of these factors was determined using the AHP, and susceptibility maps were prepared using IV and hybrid IV-AHP models. Accuracy was assessed using the ROC curve and area under the curve.

**Findings:** The results identified distance to roads, slope angle, and lithology as the most conditioning factors. The AUC was 0.770 for the IV model and 0.816 for the IV-AHP model. The IV and IV-AHP models classified approximately 29% and 32% of the Firozkuh Watershed as highly and very highly susceptible, respectively.

**Conclusion:** The results show that a considerable proportion of the watershed is classified as highly susceptible to landslides. Both the IV and IV-AHP models demonstrated satisfactory predictive performance, supporting their application for landslide susceptibility assessment in the watershed. The main limitation of this study is the unavailability of several important conditioning factors, and future research should evaluate additional statistical and machine learning models.

**Keywords:** Firozkuh Watershed; Information Value; IV-AHP Model; ROC Curve; Susceptibility Mapping.

**CITATION LINKS**

[1] Ullah K., Wang Y., Fang Z., Wang L., R... [2] Mohammady M. Landslide ... [3] Rohan T., Shelef E., Mirus B., Coleman... [4] Froude M., Petley D. Global... [5] Iranian Landslide... [6] Hadian Amri M., Solaimani K., Kavian A... [7] Fatemi Aghda SM., Bagheri V., Razifard... [8] Guo Z., Guo F., Zhang U., He J., Li G.... [9] Chowdhury S., Rahman N., Sheik S., Say... [10] Khan H., Shafique M., Khan M.A., Bacha... [11] Wubalem A., Getahun B., Hailemariam Y.... [12] Mohammady M., Pourghasemi H.R., Pradha... [13] Alsabhan A.H., Singh K., Sharma A., Al... [14] Ercanoglu M., Gokceoglu C. Assessment ... [15] Chen W., Xie X., Wang J., Pradhan B., ... [16] 16. Achour Y., Keesstra S. How do mach... [17] Rai S.C., Pandey V.K., Sharma K.K., Sh... [18] Jiang H., Zhou H., Wu J., Liu M., Wu Y... [19] Azarafza M., Azarafza M., Akgün H., At... [20] Ado M., Amitab K.; Maji A.K., Jasińska... [21] Qazi A., Singh K., Vishwakarma D.K., A... [22] Fagbohun B.J., Aladejana O.O., Okonye ... [23] Wang Y., Kang L., Wang J. Landslide ri... [24] Ali S., Biermanns P., Haider R., Reich... [25] Asmare D., Application and validation ... [26] Vardhan, P., Kumar, R. & Kaur, S. Land... [27] Mohammadzadeh M.J., Emam J.Z., Safari ... [28] Yuvaraj R.M., Dolui B. Geographical as... [29] Sevgen E., Kocaman S., Nefeslioglu H.A... [30] Mohammady M., Pourghasemi H.R., Yousef... [31] Saha S., Majumdar P., Bera B. Deep lea... [32] Yalcin, A., Reis, S., ... [33] Sharma S., Mahajan A.K. Comparative ev... [34] Sarkar S., Kanungo D.P., Patra A.K., K... [35] Tien Bui D., Pradhan B., Lofman O., Re... [36] Bisht S., Rawat K.S., Singh S.K. Earth... [37] Dhakal D., Singh K. A Geospatial Appro... [38] Yesilnacar E.K. The application of com... [39] Wang D., Hao M., Chen... [40] Mohammady M., Davudirad A. Gully Erosi... [41] Donati L., Turrini... [42] Yang Q., Wang X., Yin J., Du A., Zhang... [43] Hadji R., K. Rais L., Gadri A., Chouab... [44] Youssef A.M., Pourghasemi H.R. Landsli... [45] Hunter G., Fell R. Travel distance ang... [46] Huang Y., Xu C., Zhang X., Xue C., Wan... [47] Huang Y., Xu C., Zhang X., Xue C., Wan... [48] Orefice S., Innocenti C. Regional asse... [49] Pourghasemi H.R., Mohammady M., Pradha... [50] Hong H. Assessing landslide susceptibi... [51] Chen W., Li Y. GIS-based evaluation of... [52] Kailas A., Shajan G., Nikhila P., Joy ... [53] Hong H., Pradhan B., Sameen M.I., Kala... [54] Kamal A.M., Hossain F., Rahman M.Z., A... [55] Islam I., Ahmed W., Rizwan M., Ullah S... [56] Lobo J.M., Jiménez-Valverde A., Real, ... [57] Reichenbach P., Rossi M., Malamud B.D.... [58] Thammaboribal P., Triapthti N., Lipilo... [59] Feizizadeh B., Blaschke T. An uncertai... [60] Mohammady M., Noor H. ... [61] Mohammady M., Amiri H. ... [62] Salehpour Jam A., Mosaffaie J., Tabata...

***Correspondence***
Address: Associate Professor, College of Natural Resources, Semnan University, Semnan, Iran.
Tel: +98 (23) 31533040
E-mail: majid.mohammady@semnan.ac.ir
ORCID: 0000-0003-1428-3374

***Article History***
Received: July 13, 2026
Revised: October 25, 2026
Accepted: October 25, 2026
Published: November 6, 2026

*Copyright© 2021, the Authors | Publishing Rights, ASPI. This open-access article is published under the terms of the Creative Commons Attribution-NonCommercial 4.0 International License which permits Share (copy and redistribute the material in any medium or format) and Adapt (remix, transform, and build upon the material) under the Attribution-NonCommercial terms.*

## Introduction

In mountainous regions, landslides are among the most common and destructive hazards, causing loss of life and economic damage [1]. Mass movements and landslides are natural hazards; however, human activities, including land-use change, urban expansion, road construction in mountainous areas, and other anthropogenic interventions, have increased landslide occurrence in recent years. These events can introduce substantial quantities of soil and sediment into river systems, thereby generating debris flows and altering sediment transport regimes [2]. Since the beginning of the 21st century, landslide magnitude and impacts have increased in many regions [3]. Human activities are responsible for a substantial proportion of fatal landslides, and the frequency of such events has increased over time [4].

According to national reports, landslides between 1982 and 2007 caused 187 fatalities and widespread infrastructure damage, including 6 km of railways, 252.67 km of roads, 46 km of rural roads, and 3 km of forest roads [5]. The total economic loss from mass movements, particularly landslides, during this period is estimated at 126,893 billion Rials [5]. Landslide susceptibility mapping is a key component of landslide risk management and is widely implemented using various modeling techniques. A susceptibility map identifies areas likely to experience future landslides [6]. Landslide susceptibility mapping commonly classifies terrain by its relative likelihood of landslide occurrence, with zones categorized by their degree of susceptibility [7]. Developing rapid, accurate automated landslide assessment methods is increasingly important for effective hazard mitigation and risk management, supporting stakeholders, authorities, managers, and policymakers [8]. Landslide occurrence results from complex interactions among tectonic, hydrological, geomorphological, and climatic processes, geological conditions, vegetation cover, and erosion. Consequently, robust analytical models are needed to assess slope instability [2] reliably.

Although various methods have been developed for landslide susceptibility mapping, no single approach has yet been recognized as universally applicable to all study areas and environmental conditions [9]. Comparing multiple models within a given study area is essential to determine the most appropriate approach. Researchers then identify the best-performing model based on established performance metrics and predictive accuracy [9].

Because landslide assessment is important, researchers have used numerous models to assess landslide susceptibility. These include statistical approaches such as the Frequency Ratio model [10], the Index of Entropy [11], and the Weight of Evidence (WoE) model [12,13]. Other widely used methods include fuzzy logic approaches [14], logistic regression models [9], and machine learning algorithms [8,9, 15,16,17,18]. Deep learning methods [19,20].

Several studies have shown that bivariate statistical models can achieve acceptable predictive accuracy despite their methodological simplicity [10,13]. Nevertheless, a key limitation of bivariate approaches is their inability to account for the relative importance and interactions among landslide conditioning factors, as each factor is evaluated independently. Overlay analysis of the landslide inventory map with the conditioning factor maps, together with field observations, revealed that some factors

exert a substantially greater influence on landslide occurrence than others. Therefore, to produce a more reliable landslide susceptibility map, the relative importance of the conditioning factors should be taken into account. This limitation is not addressed by conventional bivariate statistical models, which assign weights to the classes of each factor independently without considering the relative importance of the factors themselves. To address this limitation, a hybrid method was used that combines the "Information Value" with the "Analytic Hierarchy Process". In this hybrid method, class weights of each factor are estimated using the IV model, while the relative significance of the factors is determined through AHP. The hybrid method can generate a susceptibility map that captures relationships between landslides and their conditioning factors while incorporating expert knowledge about their importance. A key consideration when applying hybrid susceptibility models is that their advantage becomes more evident where certain conditioning factors influence landslide occurrence far more than others. Under such conditions, incorporating the relative importance of the conditioning factors can improve the model's predictive performance. Although previous studies have integrated bivariate statistical methods with expert-based weighting, this study contributes by applying and evaluating the established IV–AHP framework in the Firoozkuh Watershed, rather than proposing a new methodology. The framework combines class-specific weights derived from the Information Value (IV) model with the relative importance of landslide-conditioning factors determined using the Analytic Hierarchy Process (AHP), thereby integrating inventory-based evidence with expert knowledge. The resulting landslide susceptibility map provides a regional basis for identifying landslide-prone areas and supporting land-use planning.

Both the IV and AHP models have been widely applied as standalone approaches in susceptibility assessment, and their predictive capabilities have been confirmed by numerous studies. For example, Alsabhan et al. [13], Qazi et al. [21], Fagbohun et al. [22], and Wang et al. [23] have successfully applied the IV model. In contrast, the AHP approach has shown reliable performance in investigations reported by Ali et al. [24], Asmare [25], and Vardhan et al. [26]. These findings highlight the potential of both methods and provide a strong basis for integrating them into a hybrid modeling framework.

In this study, the Firozkuh Watershed was chosen as the study area. The northern part of this watershed shows high landslide susceptibility due to complex geology, high rainfall, steep slopes, and land-use changes, particularly from road construction. Furthermore, one of Iran's principal transportation routes, connecting the capital city to Mazandaran Province, passes through the watershed, increasing its strategic importance.

## Materials & Methods

### Study Area

The Firozkuh Watershed is located in eastern Tehran Province. The Watershed covers about 1,450 $km^2$ and extends between 35°40′ and 35°57′ N latitude and 52°19′ and 53°07′ E longitude (Figure 1). This watershed is characterized by mountainous terrain, with elevation ranging from 1,712 to 3,941 m. The watershed includes the cities of Firozkuh and Arjmand. The region

has a semi-arid climate and belongs to the Turanian climatic zone [27]. The Firozkuh Watershed comprises four major land-use categories: rangeland, agriculture, residential areas, and bare land, with rangeland representing the dominant land-use type. In this watershed, landslides are a major contributor to soil erosion due to climatic, hydrological, and topographic conditions.

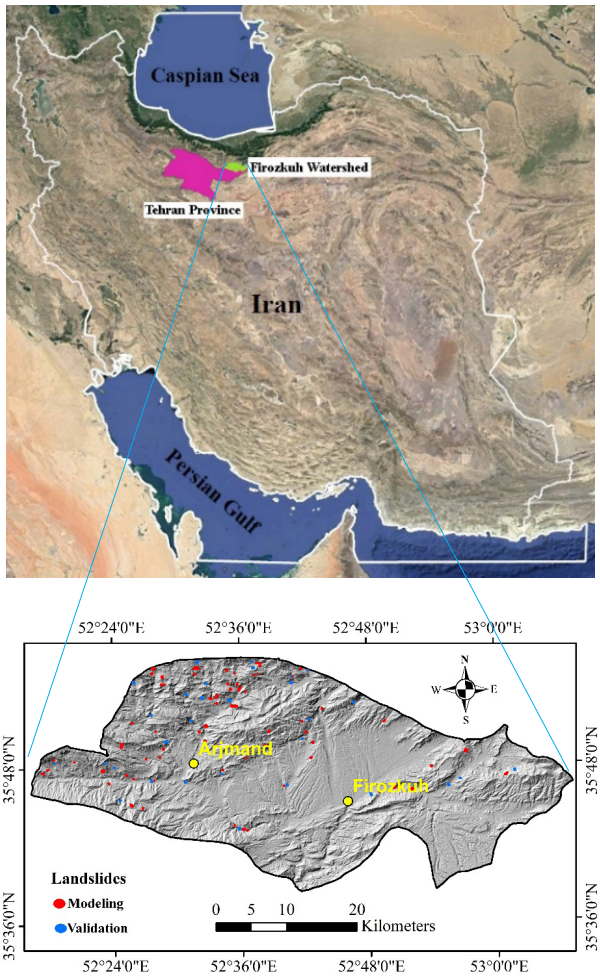



**Figure 1)** Location of the Firozkuh Watershed in Tehran and Iran.

## Methodology

The methodology of this study consists of four steps: (1) preparing a landslide inventory map; (2) creating maps of effective factors on landslide susceptibility and determining their relative importance using the AHP; (3) landslide susceptibility mapping using IV and IV-AHP approaches; and (4) assessing the accuracy of the models to identify the most appropriate model in the Firozkuh Watershed. Figure 2 presents the research methodology flowchart.

### Data Preparation

### Landslide Inventory Mapping

The Tehran Provincial Department of Natural Resources and Watershed Management prepared the preliminary landslide map. We then verified, updated, and completed this inventory map using high-resolution Google Earth imagery and extensive field investigations. Because different types of mass movements are controlled by distinct mechanisms and conditioning factors, we recorded and included only landslide occurrences in the inventory. Based on extensive field surveys conducted throughout the study area, it is believed that nearly all existing landslides were identified and included in the inventory. However, the available landslide inventory does not include landslide occurrence dates. Consequently, information regarding the timing of landslide events was not included in the landslide inventory map. A total of 102 landslides were identified within the study area, with individual landslide areas ranging from 700 to 105,000 $m^2$. To develop and validate the susceptibility models, 70% of the landslides in the inventory map were randomly selected for modeling, and 30% for validation [2]. To minimize the risk of overestimating model performance due to spatial autocorrelation, we imposed a minimum separation distance of 3 km between the training and validation datasets. Figure 3 shows examples of landslides in the study area.

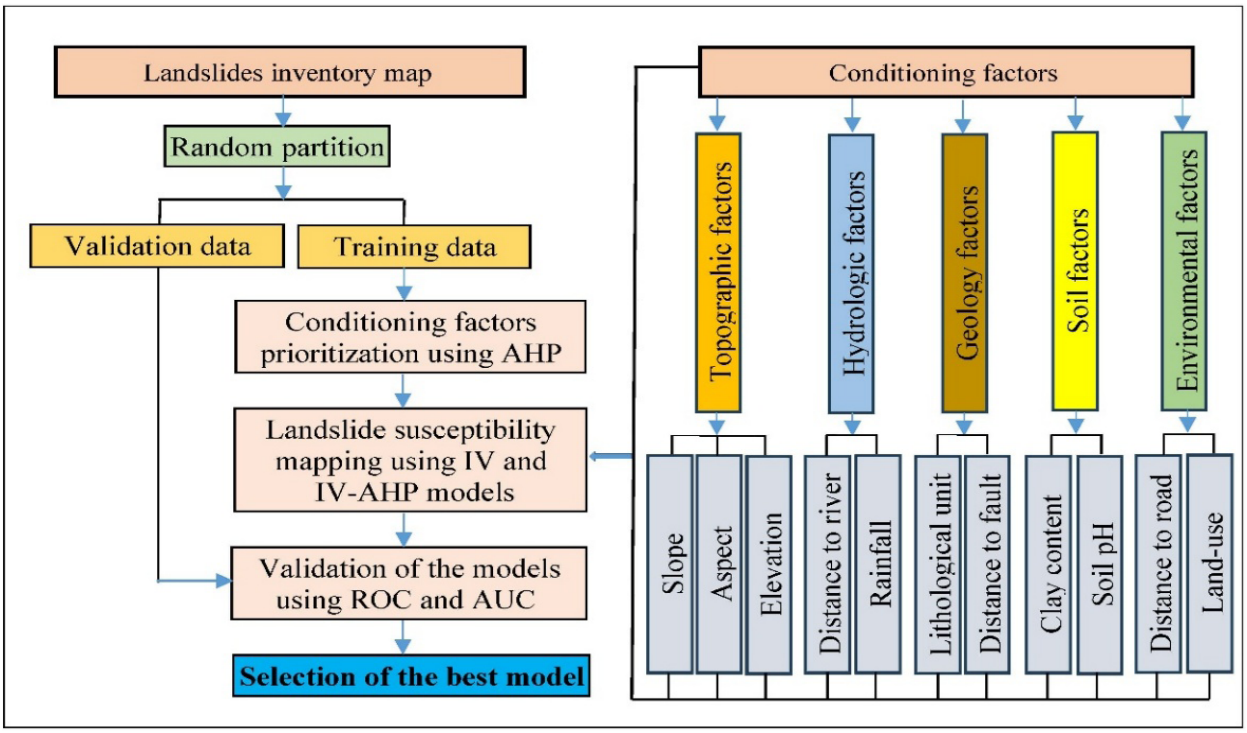



**Figure 2)** The flowchart of the research process for the landslide susceptibility mapping.



**Figure 3)** Examples of landslides in the Firozkuh Watershed.

## Data Collection

The number of factors used for landslide susceptibility assessment is not standardized, as it varies with landslide characteristics, landscape conditions, and input data quality [2]. Select factors based on their comprehensiveness, practical relevance, physical significance, measurability, and relative independence [28]. Following a comprehensive literature review [8, 9, 12, 17], field surveys, and an assessment of data availability, we selected and incorporated eleven factors into the spatial database (Figure 4). The selected factors include geological variables (lithology and distance to faults), topographic variables (slope angle, elevation, and aspect), soil properties (clay content and pH), proximity-related variables (distance to roads and rivers), land-use, and rainfall, all of which are widely recognized as important factors influencing landslide susceptibility. Although additional conditioning factors may be used in different landslide susceptibility studies, this study aimed to select representative factors from the major categories of topography, geology, soil, and land cover. The selected

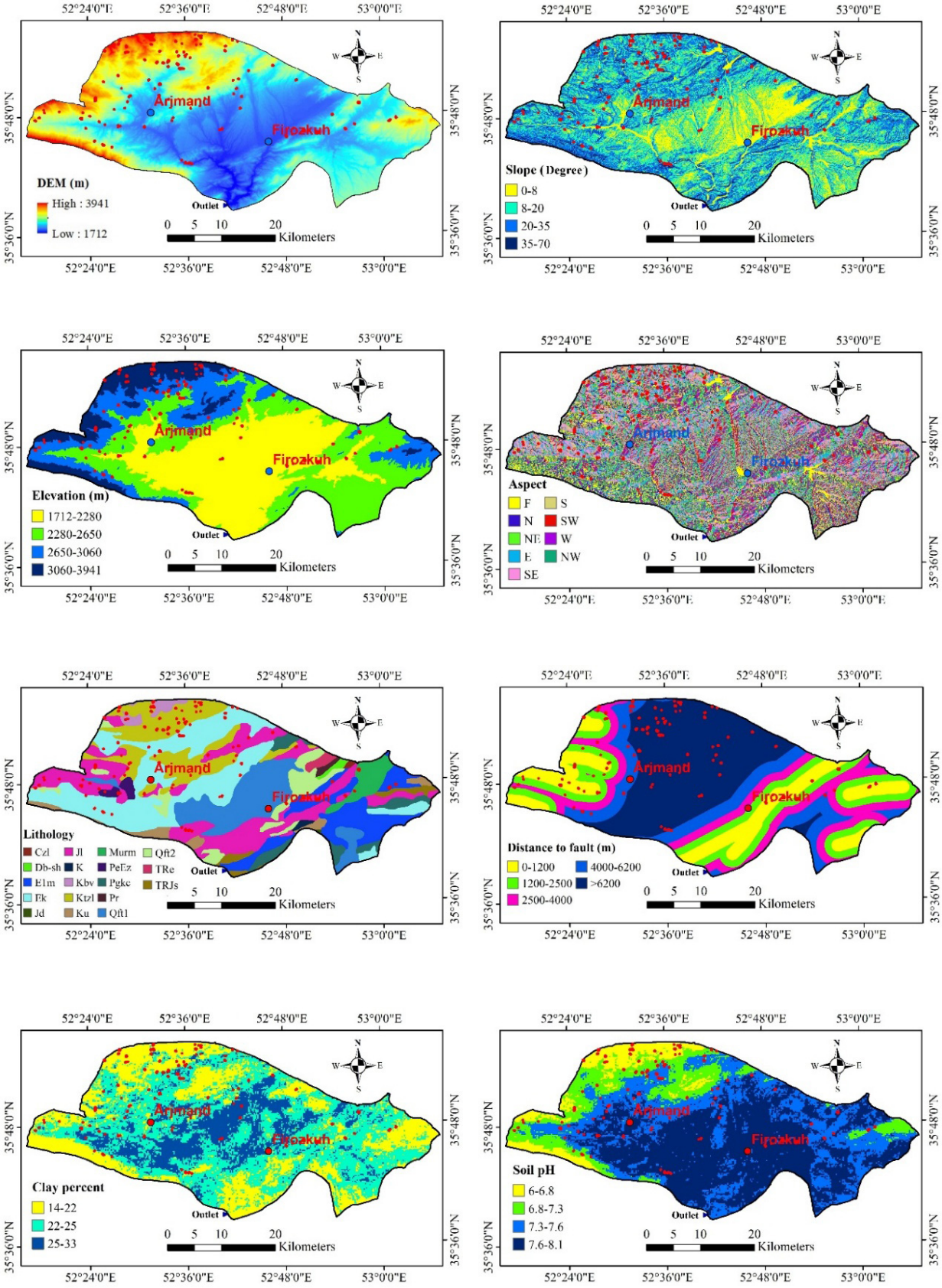



**Figure 4)** Maps of landslide conditioning factors in the Firozkuh Watershed.

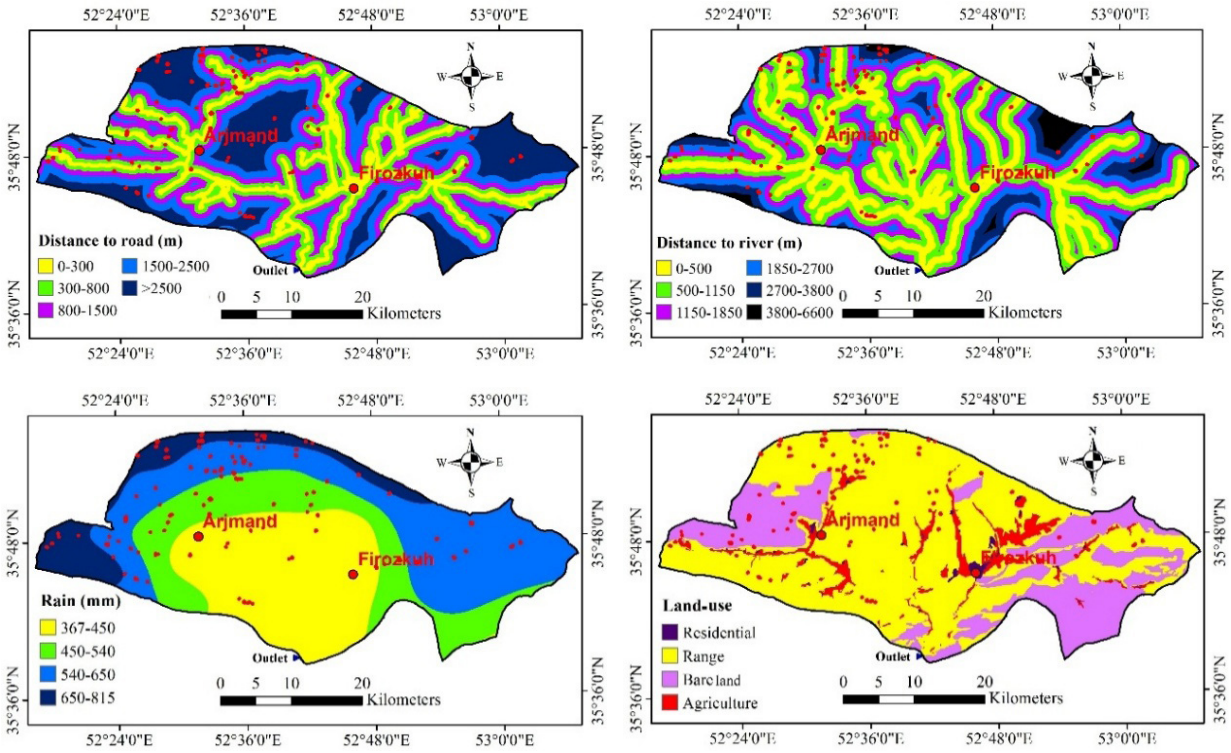



**Figure 4)** Maps of landslide conditioning factors in the Firozkuh Watershed.

factors were chosen because previous studies frequently identified them as important contributors to landslide occurrence and because they represent their respective environmental characteristics. We also considered data availability and quality when selecting the conditioning factors.

A DEM map was derived from a digitized 1:25,000-scale topographic map. We did not use the DEM directly as model input; we used it only to generate the other maps. Elevation strongly controls environmental conditions, including temperature, precipitation patterns, and human activities (land-use changes and road construction), all of which influence landslides. Using the 10 m resolution DEM, topographic variables including slope angle, aspect, and elevation class were generated. Slope angle is a key conditioning factor in landslide assessment because it strongly affects slope stability and the mechanisms that govern landslide initiation and propagation. Aspect influences the distribution of temperature, moisture, solar radiation, and vegetation cover, which in turn affect landslide occurrence [29]. The stream network was extracted from a 1:25,000-scale topographic map, and the map of distance to streams was generated using the Euclidean Distance tool in ArcGIS 9.8 software. Distances to faults and roads were also calculated using the Euclidean Distance tool in ArcGIS 10.8. The land-use map was derived from Landsat imagery with a 30-m spatial resolution acquired in 2023. A lithological map (1:100,000 scale) was generated in a GIS environment based on geological map data provided by the Geological Survey of Iran. We collected soil samples at a depth of 30 cm and analyzed them in the laboratory to determine clay content and soil pH [30]. We prepared the soil map using 30 soil samples and the Inverse Distance Weighting (IDW) interpolation

technique [30]. The rainfall distribution map was generated using precipitation data from 11 meteorological stations provided by the Iran Meteorological Organization and interpolated using the IDW method. All of the conditioning factor maps were classified using the natural break method [31].

**Prioritization of landslide conditioning factors using AHP**

The AHP derives the weights of the conditioning factors through pairwise comparisons. Each criterion was evaluated using the nine-point fundamental scale, with values ranging from 1 to 9 [32-34]. To enhance the reliability of the pairwise comparison results, the comparisons were performed by five experts with relevant expertise in landslide studies, and the aggregated expert judgments were used to construct the final pairwise comparison matrix (Table 1). In this study, we did not independently assign individual judgments and then average or sum them. Instead, all five experts jointly discussed the appropriate weight for each conditioning factor. Each expert presented and explained their opinion, and after considering the other experts' views, the group reached consensus on a single weight for each factor. The group applied this consensus-based procedure consistently to all conditioning factors. Finally, the group entered the pairwise matrix into Expert Choice 11 software (Expert Choice Inc., Arlington, VA, USA) to calculate the final factor weights. Using these weights, all conditioning factors were prioritized according to their relative importance.

**Susceptibility Mapping**

**Information Value (IV)**

The IV is a statistical model widely used for landslide susceptibility mapping [34]. Equation (1) describes the Information Value Model.

$$IV=\ln\frac{Densclass}{Densmap}=\ln\frac{\frac{Npix(Si)}{Npix(Ni)}}{\frac{SNpix(Si)}{SNpix(Ni)}} \quad \text{Eq. (1)}$$

where IV denotes the information value of a conditioning factor class; Npix(Si) shows the number of landslide pixels within class; Npix(Ni) shows the total number of pixels in class; SNpix(Si) is the total number of landslide pixels in the study area; and SNpix(Ni) is the total number of pixels in the study area [32]. In this step, the conditioning factor weights were calculated using 70% of the landslide inventory, randomly selected for model training. The remaining 30% was withheld for independent validation and was not used in the weight calculation. It should be noted that, to account for differences in landslide area, the landslides were converted into raster maps, and the number of pixels within each landslide polygon was used as an input to the model.

**Hybrid IV-AHP Model**

In the proposed hybrid model, the AHP derived the factor weights. The weight of each conditioning factor class was calculated using the Information Value (IV) method. The AHP-derived weight for each conditioning factor was multiplied by the corresponding class weight from the Information Value model to calculate the final class weights. These weights were subsequently assigned to the corresponding thematic maps. Finally, the landslide susceptibility map was produced in the GIS environment by overlaying and integrating the weighted factor maps.

**Accuracy Assessment**

Approximately 70% of the recorded landslides were used to develop the landslide

**Table 1)** Pairwise comparison matrix of landslide conditioning factors in the Firozkuh Watershed.

| Variable | Slope | Elevation | Aspect | Road | Fault | Stream | Lithology | Rain | Clay | Land-Use | Soil pH |
|---|---|---|---|---|---|---|---|---|---|---|---|
| **Slope** | 1 | 3 | 9 | 0.5 | 4 | 3 | 2 | 4 | 5 | 7 | 6 |
| **Elevation** | 0.33 | 1 | 6 | 0.33 | 3 | 2 | 0.5 | 3 | 4 | 6 | 5 |
| **Aspect** | 0.11 | 0.17 | 1 | 0.11 | 0.20 | 0.20 | 0.14 | 0.20 | 0.33 | 0.50 | 0.50 |
| **Road** | 2 | 2 | 2 | 1 | 5 | 4 | 3 | 6 | 7 | 8 | 7 |
| **Fault** | 0.25 | 0.33 | 5 | 0.20 | 1 | 0.50 | 0.33 | 2 | 3 | 5 | 3 |
| **Stream** | 0.33 | 0.50 | 5 | 0.25 | 2 | 1 | 0.50 | 3 | 3 | 5 | 4 |
| **Lithology** | 0.50 | 2 | 7 | 0.33 | 3 | 2 | 1 | 4 | 5 | 6 | 6 |
| **Rain** | 0.25 | 0.33 | 5 | 0.17 | 0.50 | 0.33 | 0.25 | 1 | 2 | 3 | 3 |
| **Clay** | 0.20 | 0.25 | 3 | 0.14 | 0.33 | 0.33 | 0.20 | 0.50 | 1 | 3 | 2 |
| **Land-use** | 0.14 | 0.17 | 2 | 0.12 | 0.20 | 0.20 | 0.17 | 0.33 | 0.33 | 1 | 0.50 |
| **Soil pH** | 0.17 | 0.20 | 2 | 0.14 | 0.33 | 0.25 | 0.17 | 0.33 | 0.50 | 2 | 1 |

susceptibility models, and the remaining 30% were applied to validate the models. For model development and validation, non-landslide samples were randomly selected across the study area. To minimize spatial dependence, a minimum separation distance of 3 km was maintained between landslide and non-landslide samples. The validation results provided an independent assessment of the predictive performance [35]. The ROC curve was generated using Eq. (2)

$$AUC = \frac{\sum TP + \sum TN}{PN} \quad \text{Eq. (2)}$$

where P and N denote the numbers of landslide (positive) and non-landslide (negative) samples, respectively. TP (true positives) and TN (true negatives) show the number of correctly classified landslide and non-landslide samples, respectively [36]. We used the Landslide Density Index (LDI) as an additional measure to validate the maps. This index is calculated by dividing the landslide density in the high and very high susceptibility classes by the landslide density in the remaining susceptibility classes. A higher value indicates higher predictive accuracy [37].

## Findings

### IV model

Based on the IV model, the weights of all classes within the conditioning factors were calculated, and the obtained results are presented in Table 2.

### AHP model

The results indicated that distance to roads received the highest weight (0.264), followed by slope angle (0.193), lithology (0.142), elevation (0.113), distance to rivers (0.085), distance to faults (0.063), rainfall (0.047), clay content (0.034), soil pH (0.025), land-use (0.019), and slope aspect (0.015), indicating that the roads and topographic conditions are the dominant factors controlling landslide occurrence in the Firozkuh Watershed. Furthermore, the calculated consistency ratio (CR) was 0.04, indicating acceptable consistency in the pairwise comparisons and confirming the reliability of the AHP results.

### Landslide Susceptibility Maps

To generate the susceptibility map using

**Table 2)** IV and IV-AHP values of conditioning factor classes.

| Factor | Attributes | Npix(Si) | Npix(Ni) | IV | IV-AHP |
|---|---|---|---|---|---|
| Elevation/DEM (meter) | 1712-2280 | 337 | 607341 | -0.6523 | -0.0737 |
| | 2280-2650 | 530 | 519477 | -0.0432 | -0.0049 |
| | 2650-3060 | 439 | 297164 | 0.3269 | 0.0369 |
| | 3060_3941 | 409 | 178589 | 0.7653 | 0.0865 |
| Slope (degree) | 0-8 | 54 | 377828 | -2.0088 | -0.3877 |
| | 8-20 | 403 | 645527 | -0.5344 | -0.1031 |
| | 20-35 | 899 | 486174 | 0.5514 | 0.1064 |
| | 35-70 | 359 | 93042 | 1.2870 | 0.2484 |
| Aspect | F | 159 | 194830 | -0.2665 | -0.0040 |
| | N | 169 | 158590 | 0.0003 | 0.00000 |
| | NE | 143 | 156635 | -0.1544 | -0.0023 |
| | E | 260 | 206250 | 0.1683 | 0.0025 |
| | SE | 432 | 236264 | 0.5402 | 0.0081 |
| | S | 188 | 170569 | 0.0340 | 0.0005 |
| | SW | 139 | 137855 | -0.0550 | -0.0008 |
| | W | 91 | 157981 | -0.6149 | -0.0092 |
| | NW | 134 | 183597 | -0.3782 | -0.0057 |
| Distance to Road (meter) | 0-300 | 398 | 251232 | 0.3968 | 0.1047 |
| | 300-800 | 316 | 309459 | -0.0424 | -0.0112 |
| | 800-1500 | 342 | 342503 | -0.0648 | -0.0171 |
| | 1500-2500 | 254 | 328181 | -0.3195 | -0.0844 |
| | >2500 | 405 | 371196 | 0.0239 | 0.0063 |
| Distance to Stream (meter) | 0-500 | 691 | 411168 | 0.4558 | 0.0387 |
| | 500-1150 | 418 | 462124 | -0.1637 | -0.0139 |
| | 1150-1850 | 154 | 331041 | -0.8286 | -0.0704 |
| | 1850-2700 | 342 | 232956 | 0.3207 | 0.0273 |
| | 2700-3800 | 88 | 127148 | -0.4313 | -0.0367 |
| | 3800-6600 | 22 | 38134 | -0.6134 | -0.0521 |
| Distance to Fault (meter) | 0-1200 | 342 | 255834 | 0.2270 | 0.0143 |
| | 1200-2500 | 193 | 267767 | -0.3907 | -0.0246 |
| | 2500-4000 | 151 | 263705 | -0.6209 | -0.0391 |
| | 4000-6200 | 287 | 234682 | 0.1380 | 0.0087 |
| | >6200 | 742 | 580583 | 0.1820 | 0.0115 |
| Land-use | Agriculture | 34 | 95155 | -1.0924 | -0.0208 |
| | Bare land | 321 | 430963 | -0.3579 | -0.0068 |
| | Rangeland | 1360 | 1062948 | 0.1831 | 0.0035 |
| | Residential | 0 | 13505 | -9.5741 | -0.1819 |
| Rainfall (mm) | 367-450 | 177 | 513570 | -1.1285 | -0.0530 |
| | 450-540 | 359 | 364592 | -0.0788 | -0.0037 |
| | 540-650 | 791 | 553180 | 0.2943 | 0.0138 |
| | 650-815 | 388 | 171229 | 0.7547 | 0.0355 |
| Soil pH | 6-6.8 | 403 | 135276 | 1.0283 | 0.0257 |
| | 6.8-7.3 | 308 | 238168 | 0.1938 | 0.0048 |
| | 7.3-7.6 | 674 | 483996 | 0.2679 | 0.0067 |
| | 7.6-8.1 | 330 | 745131 | -0.8778 | -0.0219 |
| Clay percent | 14-22 | 740 | 515486 | 0.2982 | 0.0101 |
| | 22-25 | 683 | 759958 | -0.1701 | -0.0058 |
| | 25-33 | 292 | 327127 | -0.1769 | -0.0060 |

**Table 2 Continued)** IV and IV-AHP values of conditioning factor classes.

| Factor | Attributes | Npix(Si) | Npix(Ni) | IV | IV-AHP |
|---|---|---|---|---|---|
| Geology/Lithological Units | Czl | 0 | 2313 | -7.8096 | -1.1090 |
| | Db-sh | 0 | 6201 | -8.7958 | -1.2490 |
| | E1m | 83 | 160043 | -0.7199 | -0.1022 |
| | Ek | 339 | 390015 | -0.2035 | -0.0289 |
| | Jd | 0 | 640 | -6.5248 | -0.9265 |
| | J1 | 464 | 300617 | 0.3707 | 0.0526 |
| | K | 0 | 4185 | -8.4026 | -1.1932 |
| | Kbv | 106 | 22245 | 1.4980 | 0.2127 |
| | Ktzl | 619 | 223749 | 0.9543 | 0.1355 |
| | Ku | 0 | 39200 | -10.6397 | -1.5108 |
| | Murm | 65 | 49526 | 0.2086 | 0.0296 |
| | PeEz | 14 | 15085 | -0.1379 | -0.0196 |
| | Pgkc | 0 | 57307 | -11.0195 | -1.5648 |
| | Pr | 0 | 5716 | -8.7143 | -1.2374 |
| | Qft1 | 0 | 201217 | -12.2754 | -1.7431 |
| | Qft2 | 25 | 88464 | -1.3270 | -0.1884 |
| | TRe | 0 | 10866 | -9.3567 | -1.3287 |
| | TRjs | 0 | 25182 | -10.1972 | -1.4480 |

the IV model, all layers were classified, and the information value for all classes was calculated using Equation (1). In the hybrid approach, class weights were multiplied by the corresponding conditioning factor weights obtained through AHP. The resulting values became the final conditioning-factor class weights used for susceptibility mapping. These values were then assigned to the factor classes and integrated in ArcGIS 10.8 to produce the final susceptibility maps (Figures 5 and 6). Landslide susceptibility maps were classified into four classes using the natural break method.

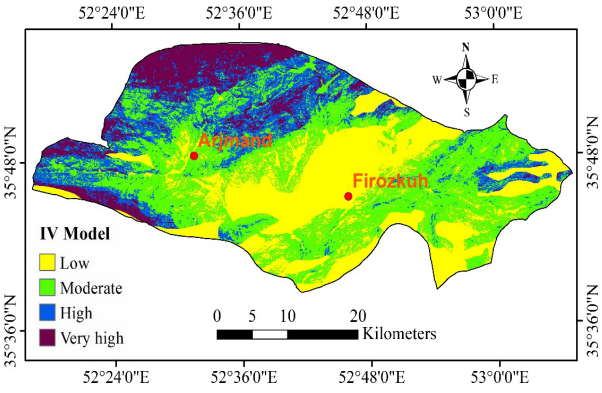



**Figure 5)** Landslide susceptibility map using the IV model.

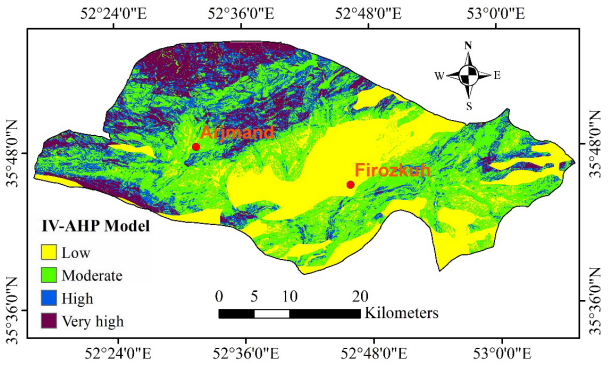



**Figure 6)** Landslide susceptibility map using the IV-AHP model.

## Accuracy Assessment

The AUC value was 0.770 for the IV model and 0.816 for the IV-AHP model (Figure 7 and Table 3). AUC values can be categorized as low (0.5-0.6), moderate (0.6-0.7), good (0.7-0.8), very good (0.8-0.9), and excellent (0.9-1.0) [38]. Accordingly, the IV model exhibited good predictive performance, whereas the IV-AHP model demonstrated very good predictive performance.

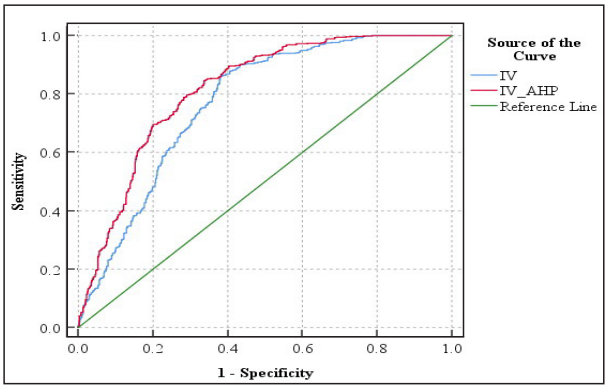



**Figure 7)** ROC curve of the IV and IV-AHP models.

**Table 3**) Statistical performance metrics for the used models.

| Model | Area | Standard Error | Asymptotic 95 % Confidence Interval | |
|---|---|---|---|---|
| | | | Lower Bound | Upper Bound |
| IV | 0.770 | 0.012 | 0.746 | 0.795 |
| IV-AHP | 0.816 | 0.011 | 0.794 | 0.838 |

The LDI values for the IV and IV-AHP models were 2.05 and 2.95, respectively. These results agreed with the ROC analysis.

The area of each landslide susceptibility class was calculated for both models (Table 4). According to the susceptibility maps, approximately 29% and 32% of the Firozkuh Watershed were classified as high and very high susceptibility by the IV and IV-AHP models.

**Table 4**) Total area of susceptibility classes for the models.

| Model | Susceptibility Classes Area ($km^2$) | | | |
|---|---|---|---|---|
| | Low | Moderate | High | Very High |
| IV | 462.4 | 557.7 | 257.3 | 164.9 |
| IV-AHP | 424.5 | 570.5 | 268.5 | 188.8 |

## Discussion

The AHP results indicated that distance to roads, slope angle, lithology, and elevation were the most important conditioning factors. Human activities, particularly road construction, have increasingly influenced landslides. Road construction alters the landscape's geomorphological structure, and slope cutting along hillsides disrupts natural slope stability. These artificial slope cuts reduce slope stability, thereby increasing the landslide occurrence in mountainous areas [39]. Road construction also alters a watershed's hydrological response, changing surface runoff patterns and accelerating soil degradation [40]. The importance of distance to roads as a key factor has also been highlighted in other studies. For example, Wang et al. [39], Donati and Turrini [41], and Yang et al. [42] identified road proximity as an important factor controlling landslide occurrence. Slope is the second most important conditioning factor influencing landslides because landslide likelihood is strongly related to slope angle [43]. Slope influences seepage processes, shear stress,

and gravitational forces, which together control slope stability and landslide occurrence [44]. Numerous previous studies have identified slope as an important conditioning factor influencing landslides [8, 17, 28, 45]. Lithology is another key conditioning factor controlling landslides. This finding is expected because lithology determines the physical and mechanical properties of slope materials [46]. It is widely recognized that lithological characteristics strongly influence the properties of materials, and consequently play a crucial role in influencing landslide occurrence [28]. Lithological characteristics have been recognized as a significant conditioning factor for landslide occurrence in numerous studies, including those by Yuvaraj and Dolui [28], Huang et al. [47], and Orefice and Innocenti [48]. Elevation indirectly influences several factors associated with landslide occurrence, including temperature, precipitation, and freeze-thaw processes [49-51]. Similarly, Guo et al. [8] and Kailas et al. [52] identified elevation as one of the most conditioning factors controlling landslide occurrence. Based on the information values calculated using the IV model (Table 2), the 3060-3941 m elevation class exhibited the highest landslide susceptibility. Low elevations in the Firozkuh Watershed have gentler slopes and therefore exhibit lower landslide susceptibility. At higher elevations, precipitation falls predominantly as snow. Subsequent snowmelt enhances water infiltration, increasing pore water pressure and promoting landslides. Landslide density across different slope classes showed that slopes steeper than 20° exhibited the highest Information Value (IV) scores. Steeper slopes reduce slope stability by increasing shear stress while decreasing the effective cohesion of soil and weathered materials, thereby promoting landslide occurrence [45]. The aspect analysis indicated that the southeastern and eastern aspects had the highest information value weights. Reduced soil moisture and sparser vegetation cover on these slopes may reduce slope stability and, consequently, increase landslide susceptibility. It should be noted that the difference in the Information Value weights between these two aspects and the remaining aspect classes is relatively small, and landslides are distributed across almost all slope aspects in the study area. This pattern suggests that slope aspect has only a limited influence on landslide occurrence compared with other conditioning factors, whose effects appear more dominant. This interpretation also aligns with the AHP results, where slope aspect received the lowest weight among all conditioning factors. The highest information value weight for the distance to stream factor was obtained for areas located within 500 m of streams. Stream erosion and groundwater-level fluctuations can reduce slope stability by undercutting slope toes and increasing soil saturation. Consequently, landslide susceptibility generally decreases with increasing distance from streams [8,17, 36]. The highest landslide susceptibility was observed within 0-300 m of roads. Road construction in steep, hilly terrain disturbs natural slope geometry, weakens the rock mass, and reduces slope stability [41]. Areas located within 1200 m of faults exhibited high susceptibility. Fault zones are generally characterized by highly fractured soil. These fractured materials have reduced mechanical strength and are therefore more susceptible to slope failure, particularly during earthquakes [42]. Among the lithological units, kbv (Basaltic volcanic), ktzl (White to

pinkish orbitolina bearing limestone), J1(Light grey, thin - bedded to massive limestone), and murm (Light-red to brown marl and gypsiferous marl with sandstone intercalations) were associated with the highest information value weights, indicating a greater susceptibility to landslide occurrence. These salt-bearing, fine-grained materials readily absorb water, reducing material strength and increasing slope instability. Consequently, these formations in the Firozkuh Watershed show higher landslide susceptibility [2]. Among the land-use categories, rangelands exhibited the highest landslide susceptibility. This pattern likely reflects that rangelands are predominantly located on steep slopes, where topographic conditions favor landslides.

Although rangelands exhibited the highest susceptibility, landslides were distributed across all land-use categories. Therefore, rangelands' relatively high susceptibility may reflect other conditioning factors, such as elevation and slope, commonly associated with this land-use type. This interpretation is supported by the AHP results, which assigned a relatively low weight to land use, indicating that it is not among the dominant conditioning factors controlling landslide occurrence in the study area. Among the rainfall classes, the 650-815 mm class had the highest IV weight. Rainfall is a major landslide factor because infiltration increases pore water pressure while reducing soil shear strength, thereby reducing slope stability and initiating slope failure [53]. Analysis of clay content and soil pH classes revealed that the 14–22% clay class and the pH class of 6–6.8 had the highest information-value weights. This pattern may be attributed to the fact that soils with low to moderate clay content generally contain higher proportions of silt and sand, resulting in greater permeability and faster rainfall infiltration. Consequently, pore water pressure can rise rapidly during intense or prolonged rainfall, reducing soil shear strength and increasing slope instability. Higher landslide occurrence in low-pH soils may be explained by enhanced weathering and dissolution of cementing materials under acidic conditions, reducing soil strength and structural stability [54]. Islam et al. [55] also support the role of soil pH as an important factor influencing landslide occurrence.

As shown in the results, both models achieved satisfactory accuracy in the Firozkuh Watershed. A major advantage of bivariate models, such as the IV model, is their ease of implementation combined with satisfactory predictive performance in landslide susceptibility mapping [13, 23, 34]. A key limitation of bivariate statistical models, such as the IV model, is that they assign weights independently to the classes of each factor without considering the relative significance of the factors themselves. Assessing the relative importance of landslide conditioning factors is essential in landslide susceptibility mapping because a dominant factor may mask the influence of others, underestimating their contribution to the final susceptibility map. To address this limitation, a hybrid IV-AHP model was developed by integrating the weights derived from the IV model with the factor weights obtained using the AHP. The IV–AHP model achieved a higher AUC (0.818) than the IV model (0.770), while the Landslide Density Index (LDI) increased from 2.05 to 2.95. These results suggest that the hybrid model provided better overall discrimination and a

stronger concentration of landslides in the higher-susceptibility classes. However, the 0.048 AUC difference is not statistically significant without a formal statistical comparison. Furthermore, because ROC-AUC measures overall discrimination but does not fully characterize the spatial distribution of prediction errors, AUC and LDI should be interpreted as complementary indicators of model performance [56,57].

A key limitation of AHP is its reliance on expert judgment in pairwise comparisons, which may introduce subjectivity and uncertainty into factor weights [58]. Although expert knowledge can incorporate local environmental conditions, differences in expert perceptions and inconsistent pairwise judgments may affect the resulting weights and, consequently, the susceptibility map. Therefore, the predictive performance of the IV–AHP model should be interpreted with these uncertainties in mind. Future studies could use sensitivity analysis to assess how robust the results are to changes in factor weights [59]. The integration of the AHP with bivariate statistical models has been adopted in previous studies, including landslide susceptibility [60] and badland erosion mapping [61]. These hybrid approaches have consistently achieved higher accuracy than bivariate models.

According to the IV and IV-AHP models, the high and very high susceptibility classes occupied approximately 29% and 32% of the Firozkuh Watershed, respectively. These results indicate that a considerable proportion of the watershed is vulnerable to landslides and should be prioritized in land-use planning. The Firozkuh Watershed is highly susceptible to landslide occurrence because of its physiographic characteristics, mountainous topography, and climatic conditions. Furthermore, the watershed is traversed by the major Tehran-Mazandaran Road, and ongoing land-use changes, particularly road construction and expansion, have further increased landslide susceptibility in the area.

A key limitation of landslide susceptibility assessment is the potential incompleteness of the landslide inventory. Although we combined Google Earth imagery with extensive field surveys to improve landslide identification, the study area's complex topography may have prevented us from detecting all landslides, introducing uncertainty into the susceptibility maps. Future studies could reduce this uncertainty by incorporating high-resolution imagery and object-based remote sensing techniques. Geospatial datasets and susceptibility maps provide valuable information for sustainable development in mountainous areas by supporting land-use planning and the identification of landslide-susceptible zones [62]. Landslides annually cause substantial damage to residential areas and infrastructure, particularly road networks. Identifying landslide-prone areas and integrating this information into land-use planning and development control effectively reduces future landslide losses.

## Conclusion

The Firozkuh Watershed is highly susceptible to landslides because of its climate, complex topography, and geology. Given the watershed's importance, particularly because the Tehran-Mazandaran road traverses it, effective landslide management is essential to reduce the risk of slope failures. In this study, we applied the IV model and a hybrid IV-AHP model to assess landslide susceptibility. The validation

results showed that both methods provided good predictive performance; however, the hybrid IV-AHP model performed better than the conventional IV model. The AHP results identified distance to roads, slope angle, lithology, and elevation as the most important factors controlling landslide occurrence. According to the IV and IV-AHP models, approximately 29% and 32% of the Firozkuh Watershed were classified into high and very high landslide susceptibility classes, respectively. These findings highlight the need to prioritize these areas in land-use planning and landslide management. One limitation of the present study is the lack of data for several potentially important landslide-conditioning factors, including soil depth, silt and sand content, and traffic volume on the regional road network. Future studies should also assess additional approaches, including multivariate statistical and data mining models, to identify the most appropriate model for the study area.

**Acknowledgments:** Not applicable.

**Author contributions:** All stages of the research have been carried out by Majid Mohammady. **Ethical Permissions:** None declared.

**Funding/ Support:** This study received no external funding.

**Conflicts of Interest:** The author declares no conflict of interest.

**AI Use Declaration:** The author used ChatGPT (https://chatgpt.com) solely for language editing. The author carefully reviewed and revised the AI-generated output and accepts full responsibility for the manuscript content.

## References

1. Ullah K., Wang Y., Fang Z., Wang L., Rahman M. 2022. Multi-hazard susceptibility mapping based on Convolutional Neural Networks. 101425 Geosci. Front. 2022; 13(5):1025.
2. Mohammady M. Landslide Susceptibility Assessment using Bivariate and Data Mining Methods. ECOPERSIA 2025; 13(4):407-427.
3. Rohan T., Shelef E., Mirus B., Coleman T. Prolonged influence of urbanization on landslide susceptibility. Landslides. 2023; 20: 1433–1447.
4. Froude M., Petley D. Global fatal landslide occurrence from 2004 to 2016. Nat. Hazard. Earth Syst. Sci. 2018; 18(8):2161–2181.
5. Iranian Landslide Working Party (ILWP) (2007). Iranian landslides list, Forest, Rangeland and Watershed Association, Iran: 13p.
6. Hadian Amri M., Solaimani K., Kavian A., Afzal P. A new approach to landslide assessment using the Depth-Number fractal model. ECOPERSIA 2023; 11(1):11-23.
7. Fatemi Aghda SM., Bagheri V., Razifard M. Landslide Susceptibility Mapping Using Fuzzy Logic System and Its Influences on Mainlines in Lashgarak Region, Tehran, Iran. Geotech. Geol. Eng. 2018; 36(2):915–937.
8. Guo Z., Guo F., Zhang U., He J., Li G., Yang Y., Zhang X. A Python system for regional landslide susceptibility assessment by integrating machine learning models and its application. Heliyon. 2023; 9(11):e21542.
9. Chowdhury S., Rahman N., Sheik S., Sayeid A., Mahmud K.H., Hafsa B. GIS-based landslide susceptibility mapping using logistic regression, random forest, and decision and regression tree models in Chattogram District, Bangladesh. Heliyon. 2024; 10(1):e23424.
10. Khan H., Shafique M., Khan M.A., Bacha M.A., Shah S.U., Calligaris C. Landslide susceptibility assessment using Frequency Ratio: a case study of northern Pakistan. Egypt J. Rem. Sens. Space Sci. 2019; 22(1):11–24.
11. Wubalem A., Getahun B., Hailemariam Y., Mesele A., Tesfaw G., Dawit Z., Goshe E. Landslide susceptibility modeling using the index of entropy and frequency ratio method from Nefas-Mewcha to Weldiya Road corridor, northwestern Ethiopia. Geotech. Geol. Eng. 2022; 40(10):5249–5278.
12. Mohammady M., Pourghasemi H.R., Pradhan B. Landslide susceptibility mapping at Golestan Province, Iran: a comparison between frequency ratio, Dempster-Shafer, and weights of evidence models. J. Asian Earth Sci. 2012; 61(1):221–236.
13. Alsabhan A.H., Singh K., Sharma A., Alam S., Pandey D.D., Rahman S.A.S., Khursheed A., Munshi F.M. Landslide susceptibility assessment in the Himalayan range based along Kasauli–Parwanoo road corridor using weight of evidence, information value, and frequency ratio.

J. King Saud. Univ. Sci. 2022; 34(2):101759.
14. Ercanoglu M., Gokceoglu C. Assessment of landslide susceptibility for a landslide-prone area (north of Yenice, NW Turkey) by fuzzy approach. Environ. Geol. 2002; 41(6):720–730.
15. Chen W., Xie X., Wang J., Pradhan B., Hong H., Bui DT., Duan Z., Ma J. A comparative study of logistic model tree, random forest, and classification and regression tree models for spatial prediction of landslide susceptibility. Catena 2017; 151(1):147–160.
16. Achour Y., Keesstra S. How do machine learning techniques help in increasing accuracy of landslide susceptibility maps? Geosci. Front. 2020; 11(3):871-883.
17. Rai S.C., Pandey V.K., Sharma K.K., Sharma S. Landslide susceptibility analysis in the Bhilangana Basin (India) using GIS-based machine learning methods. Geosystems Geoenvironment. 2024; 3(2):100253.
18. Jiang H., Zhou H., Wu J., Liu M., Wu Y., Guo Y. Ensemble learning for landslide susceptibility mapping: a review of machine learning and hybrid approaches. Carbonates Evaporites. 2026; 41(1):16.
19. Azarafza M., Azarafza M., Akgün H., Atkinson P.M., Derakhshani R. Deep learning-based landslide susceptibility mapping. Sci. Rep. 2021; 11(1):24112.
20. Ado M., Amitab K.; Maji A.K., Jasińska E., Gono R., Leonowicz Z., Jasiński M. Landslide Susceptibility Mapping Using Machine Learning: A Literature Survey. Remote Sens. 2022; 14(13):3029.
21. Qazi A., Singh K., Vishwakarma D.K., Abdo H.G. GIS-based landslide susceptibility zonation mapping using frequency ratio, information value, and weight of evidence: a case study in Kinnaur District, HP, India. Bull. Eng. Geol. Environ. 2023;82(8):332.
22. Fagbohun B.J., Aladejana O.O., Okonye I.F., Tobore A.O. Assessing gully erosion susceptibility dynamics using information value and hazard index methods: A case study of Agulu-Nanka watershed, Southeast Nigeria. Catena. 2024; 241(1):108070.
23. Wang Y., Kang L., Wang J. Landslide risk assessment combining kernel extreme learning machine and information value modeling-A case study of Jiaxian County of the Loess Plateau, China. Heliyon. 2024; 10(17):e37352.
24. Ali S., Biermanns P., Haider R., Reicherter K. Landslide susceptibility mapping using GIS along CPEC (Karakoram Highway), Pakistan. Nat. Hazards Earth Syst. Sci. 2019; 19(5):999–1022.
25. Asmare D., Application and validation of AHP and FR methods for landslide susceptibility mapping around Choke Mountain, northwestern Ethiopia. Sci. Afr. 2023; 19(1):e01470.
26. Vardhan P., Kumar R. Kaur S. Landslide Susceptibility Mapping of Pithoragarh, India Using Analytical Hierarchy Process and Support Vector Machine. Natl. Acad. Sci. Lett. 2026; 1(1):1-9.
27. Mohammadzadeh M.J., Emam J.Z., Safari M., Mousavi M., Ghanbarzadeh B., Philips G.O. Physicochemical and emulsifying properties of Barijeh (*Ferula gumosa*) Gum. Iran J Chem Chem Eng. 2007; 26(3):81–88.
28. Yuvaraj R.M., Dolui B. Geographical assessment of landslide susceptibility using a statistical approach. Quat. Sci. Adv. 2023; 11:100097.
29. Sevgen E., Kocaman S., Nefeslioglu H.A., Gokceoglu C.A. Novel performance assessment approach using photogrammetric techniques for landslide susceptibility mapping with logistic regression, ANN, and random forest. Sensors. 2019; 19(18):3940.
30. Mohammady M., Pourghasemi H.R., Yousefi S., Dastres E., Edalat M., Pouyan S., Eskandari S. Modeling and prediction of habitat suitability for Ferula gummosa medicinal plant in a mountainous area. Nat. Resour. Res. 2021; 30(6):4861–4884.
31. Saha S., Majumdar P., Bera B. Deep learning and benchmark machine learning-based landslide susceptibility investigation, Garhwal Himalaya (India). Quat. Sci. Adv. 2023; 10(1):100075.
32. Yalcin, A., Reis, S., Aydinoglu, A.C., Yomralioglu, T. A GIS-based comparative study of frequency ratio, analytical hierarchy process, bivariate statistics and logistic regression methods for landslide susceptibility mapping in Trabzon, NE Turkey, Catena. 2011; 85(3):274–287.
33. Sharma S., Mahajan A.K. Comparative evaluation of GIS-based landslide susceptibility mapping using statistical and heuristic approach for Dharamshala region of Kangra Valley, India, Geoenviron. Disasters. 2018;5(1):1–16.
34. Sarkar S., Kanungo D.P., Patra A.K., Kumar P. GIS-based spatial data analysis for landslide susceptibility mapping. J. Mt. Sci. 2008; 5(1):52–62.
35. Tien Bui D., Pradhan B., Lofman O., Revhaug I. Landslide susceptibility assessment in Vietnam using support vector machines, decision tree, and Naive Bayes models. Math. Probl. Eng. 2012; 1(1):1–26.
36. Bisht S., Rawat K.S., Singh S.K. Earth observation data and GIS-based landslide susceptibility analysis through frequency ratio model in the Lesser Himalayan region, India. Quat. Sci. Adv. 2024;13(1):100141.
37. Dhakal D., Singh K. A Geospatial Approach to Landslide Susceptibility Mapping of Spiti, India. J. Min. Environ. 2025; 16(1): 183-205.
38. Yesilnacar E.K. The application of computational

intelligence to landslide susceptibility mapping in Turkey. PhD Thesis, Department of Geomatics, the University of Melbourne. 2005. p 423.
39. Wang D., Hao M., Chen S., Meng Z., Jiang D., Ding F. Assessment of landslide susceptibility and risk factors in China. Nat. Hazard. 2021; 108(3):3045–3059.
40. Mohammady M., Davudirad A. Gully Erosion Susceptibility Assessment Using Different Machine Learning Algorithms: A Case Study of Shazand Watershed in Iran. Environ. Model. Assess. 2024; 29(2):249–261.
41. Donati L., Turrini M.C. An objective method to rank the importance of the factors predisposing to landslides with the GIS methodology: application to an area of the Apennines (Valnerina; Perugia, Italy). Eng. Geol. 2002; 63(3-4): 277–289.
42. Yang Q., Wang X., Yin J., Du A., Zhang A., Wang L., Guo H., Li D. A novel CGBoost deep learning algorithm for coseismic landslide susceptibility prediction. Geosci. Front. 2024; 15(2):101770.
43. Hadji R., K. Rais L., Gadri A., Chouabi Y., Hamed. Slope failure characteristics and slope movement susceptibility assessment using GIS in a medium scale: a case study from Ouled Driss and Machroha municipalities, Northeast Algeria. Arab. J. Sci. Eng. 2017; 42(1):281–30.
44. Youssef A.M., Pourghasemi H.R. Landslide susceptibility mapping using machine learning algorithms and comparison of their performance at Abha Basin, Asir Region, Saudi Arabia. Geosci. Front. 2021; 12(2):639–655.
45. Hunter G., Fell R. Travel distance angle for "rapid" landslides in constructed and natural soil slopes. Can. Geotech. J. 2003; 40(6):1123–1141.
46. Huang Y., Xu C., Zhang X., Xue C., Wang S. An updated database and spatial distribution of landslides triggered by the Milin, Tibet Mw6.4 Earthquake of 18 November 2017, J. Earth Sci. 2021; 32(5):1069–1078.
47. Huang Y., Xu C., Zhang X., Xue C., Wang S. 2021. An updated database and spatial distribution of landslides triggered by the Milin, Tibet Mw6.4 Earthquake of 18 November 2017. J. Earth Sci. 2021; 32(5):1069–1078.
48. Orefice S., Innocenti C. Regional assessment of coastal landslide susceptibility in Liguria, Northern Italy, using MaxEnt. Nat. Hazard. 2025; 121(3):2613–2639.
49. Pourghasemi H.R., Mohammady M., Pradhan B. Landslide susceptibility mapping using index of entropy and conditional probability models in GIS: Safarood Basin, Iran. Catena. 2012; 97(3): 71–84.
50. Hong H. Assessing landslide susceptibility based on a hybrid Best-first decision tree with an ensemble learning model. Ecol. Indic. 2023; 147(1):109968.
51. Chen W., Li Y. GIS-based evaluation of landslide susceptibility using hybrid computational intelligence models. Catena. 2020; 195(1):104777.
52. Kailas A., Shajan G., Nikhila P., Joy S., George G.K., Prakash V. Landslide hazard zonation (LHZ) mapping of Attappady, Kerala using GIS. Int. Res. J. Eng. Technol. 2018;5(3):3808–3812.
53. Hong H., Pradhan B., Sameen M.I., Kalantar B., Zhu A., Chen W. Improving the accuracy of landslide susceptibility model using a novel region-partitioning approach. Landslides. 2018; 15(4):753–772.
54. Kamal A.M., Hossain F., Rahman M.Z., Ahmed B., Sammonds P. Geological and soil engineering properties of shallow landslides occurring in the Kutupalong Rohingya Camp in Cox's Bazar, Bangladesh. Landslides. 2022; 19(2):465–478.
55. Islam I., Ahmed W., Rizwan M., Ullah S., Orakzai A.U., Petrounias P. Investigating the role of geochemistry and geotechnical properties in landslide characterization and triggering mechanisms: A case study from Dir Upper, Khyber Pakhtunkhwa, Pakistan. Phys. Chem. Earth. 2024; 135(1):103636.
56. Lobo J.M., Jiménez-Valverde A., Real, R. AUC: A misleading measure of the performance of predictive distribution models. Glob. Ecol. Biogeogr. 2008; 17(2):145–151.
57. Reichenbach P., Rossi M., Malamud B.D., Mihir M., Guzzetti F. A review of statistically-based landslide susceptibility models. Earth-Sci. Rev. 2018;180(1):60–91.
58. Thammaboribal P., Triapthti N., Lipiloet S. Using of Analytical Hierarchy Process (AHP) in Disaster Management: A Review of Flooding and Landslide Susceptibility Mapping. Int. J. Geoinform. 2025; 21(4):177–196.
59. Feizizadeh B., Blaschke T. An uncertainty and sensitivity analysis approach for GIS-based multicriteria landslide susceptibility mapping. Int. J. Geogr. Inf. Sci. 2014; 28(3): 610–638.
60. Mohammady M., Noor H. Landslide Susceptibility Zoning Using New Synthetic Method in the GIS Environment. J. Env. Sci. Tech. 2020; 21(12):1-12. (In Persian).
61. Mohammady M., Amiri H. Prioritizing Effective Factors and Badland Erosion Susceptibility Assessment Using Synthetic Model of Information Value and AHP. Iran. J. Wate. Manag. Sci. 2024; 18(66):38-48. (In Persian).
62. Salehpour Jam A., Mosaffaie J., Tabatabaei M.R. Raster-based landslide susceptibility mapping using compensatory MADM methods. Environ. Model. Softw. 2023; 159(1):105567